Supporting Information

Defect-engineered VO_x cathode and novel polyvinyl alcohol@polyaniline hydrogel separator for ultra-stable fiber Zn-ion batteries

Yahui Zhang, Juan Xu*, Yuezhou Jing, Mengge Ding, Jiayi Li, Pibin Bing*, Zhongyang Li*

School of Electrical Engineering, North China University of Water Resources and Electric Power, Zhengzhou 450003, P. R. China

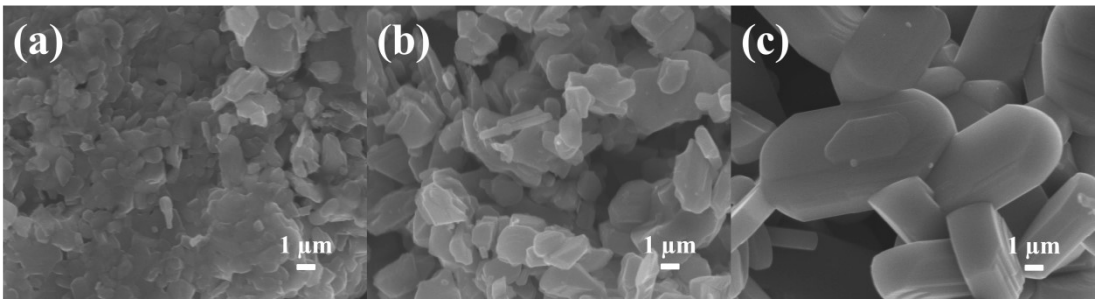

Fig S1. SEM images of (a) VO@280; (b) VO@350; (c) VO@450 composites.

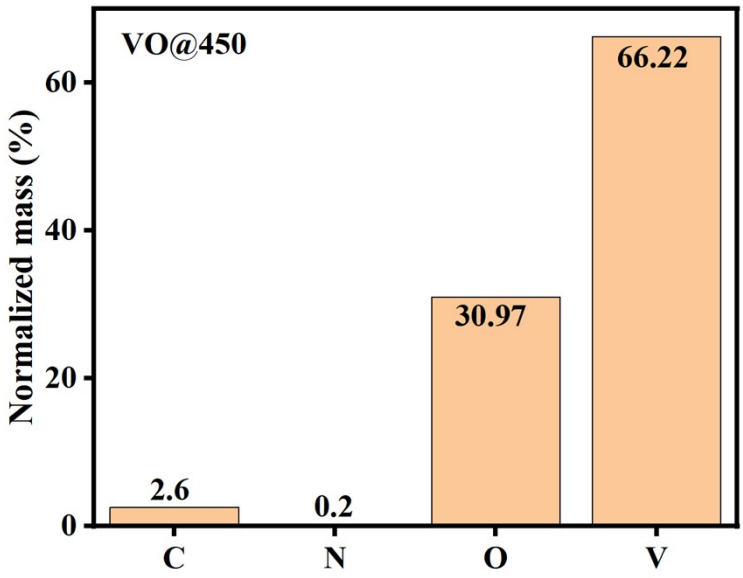

Fig S2. Normalized mass proportion of N element in VO@450 materials.

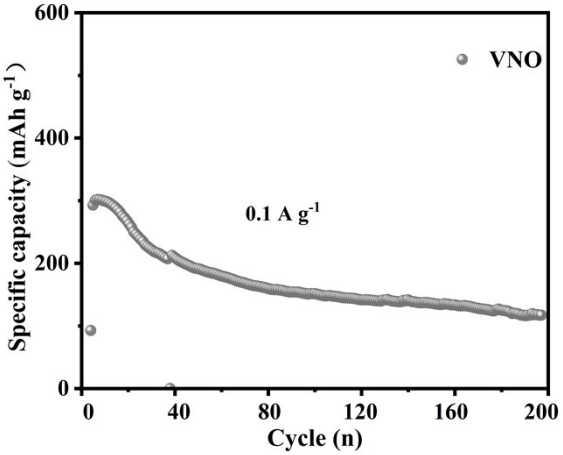

Fig S3. Cycling performance of VNO electrode at 0.1 A g^{-1}.

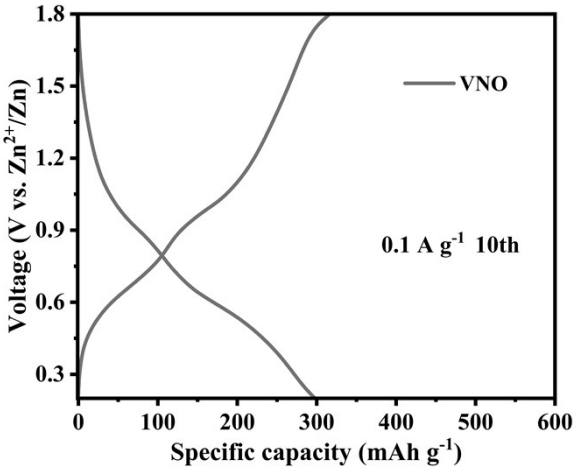

Fig S4. GCD curves of VNO electrode for the 10th turn at 0.1 A g^{-1}.

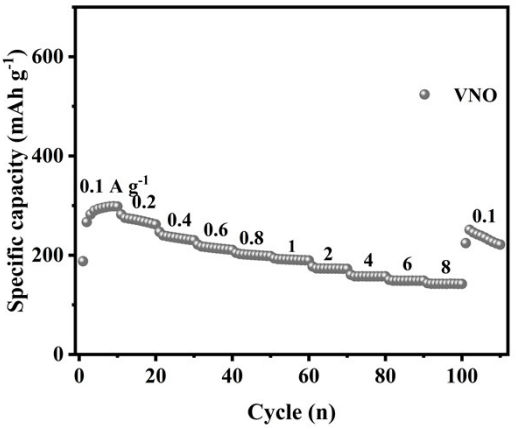

Fig S5. Rate performance of VNO electrode.

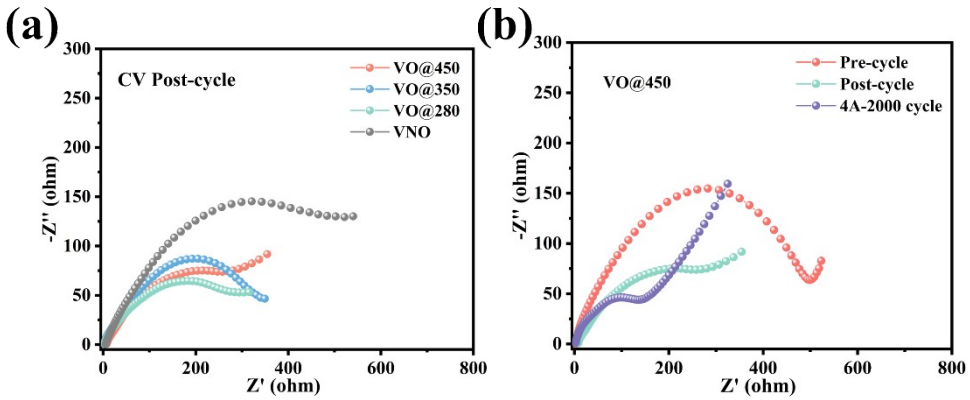

Fig S6. EIS curves: (a) After the CV tests; (b) Different stages of the VO@450 electrode.

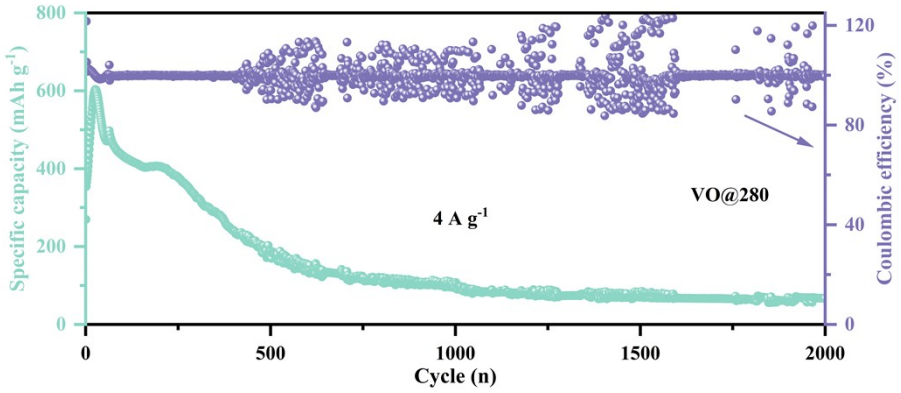

Fig S7. Long cycle performance of VO@280 electrodes at 4 A g^{-1}.

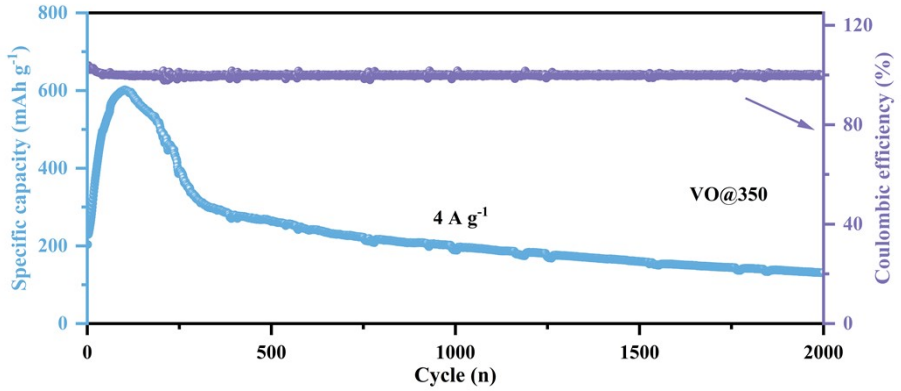

Fig S8. Long cycle performance of VO@350 electrodes at 4 A g^{-1}.

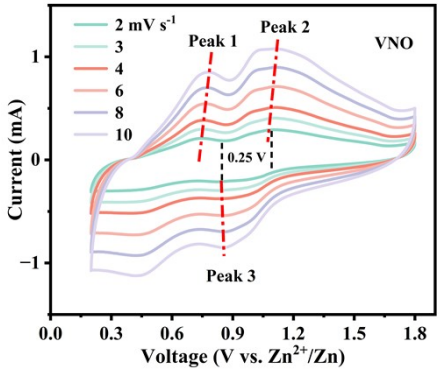

Fig S9. CV curves of the VNO electrode at varied scan rates.

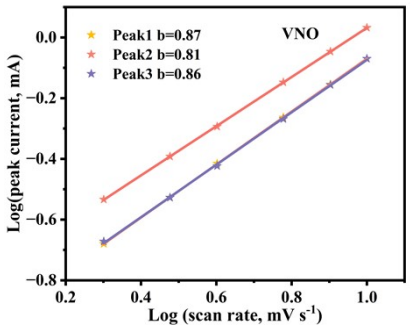

Fig S10. Plots of log(i) vs log(v) at specific peak currents for the VNO electrode.

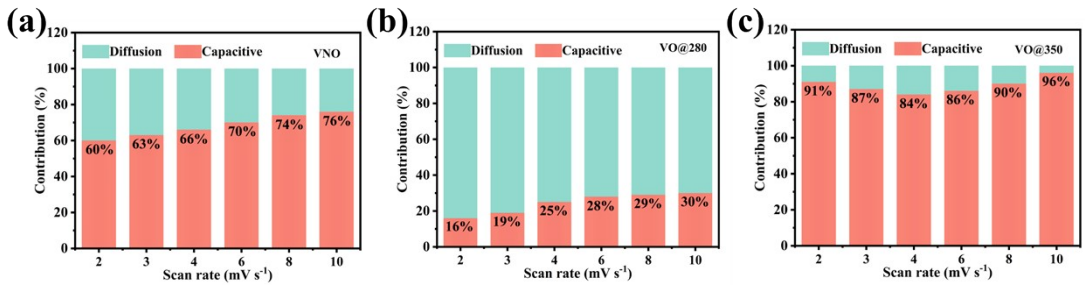

Fig S11. Capacitive and diffusion contribution at different scan rates of (a) VNO; (b) VO@280; (c) VO@350 electrodes, respectively.

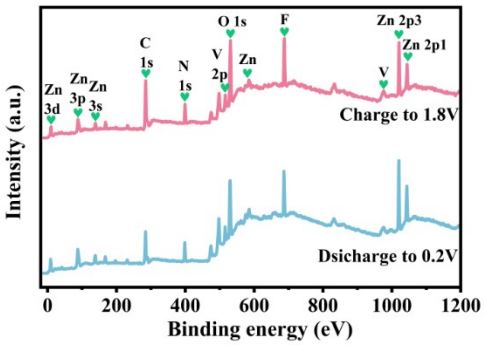

Fig S12. XPS full spectrum of VO@450 electrode at different charging/discharging states.

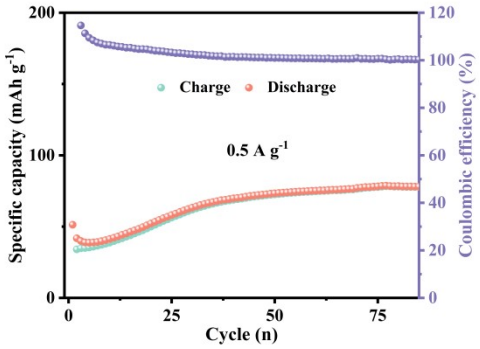

Fig S13. Cycling performance of the VO@450 based fiber zinc ion battery with PVA hydrogel separator at 0.5 A g^{-1}.